Size exclusion experiment in a grassland field unravels top-down control of the soil fauna on microbial community assembly

Mathilde Jeanbille, Sana Romdhane, Marie-Christine Breuil, David Bru, Stefan Geisen, Arnaud Mounier, Aymé Spor, Laurent Philippot

▶ **To cite this version:**

Mathilde Jeanbille, Sana Romdhane, Marie-Christine Breuil, David Bru, Stefan Geisen, et al.. Size exclusion experiment in a grassland field unravels top-down control of the soil fauna on microbial community assembly. Ecology Letters, 2024, 27 (6), pp.e14442. 10.1111/ele.14442 . hal-04674236

HAL Id: hal-04674236
https://hal.inrae.fr/hal-04674236v1

Submitted on 21 Aug 2024

HAL is a multi-disciplinary open access archive for the deposit and dissemination of scientific research documents, whether they are published or not. The documents may come from teaching and research institutions in France or abroad, or from public or private research centers.

L'archive ouverte pluridisciplinaire **HAL**, est destinée au dépôt et à la diffusion de documents scientifiques de niveau recherche, publiés ou non, émanant des établissements d'enseignement et de recherche français ou étrangers, des laboratoires publics ou privés.

Size exclusion experiment in a grassland field unravels top-down control of the soil fauna on microbial community assembly

Mathilde Jeanbille[1], Sana Romdhane[1], Marie-Christine Breuil[1], David Bru[1], Stefan Geisen[2], Arnaud Mounier[1], Aymé Spor[1], Laurent Philippot[1] *

[1] University Bourgogne Franche Comte, INRAE, Institut Agro Dijon, Department of Agroecology, Dijon, France

[2] Laboratory of Nematology, Wageningen University & Research, Wageningen, The Netherlands

* corresponding author: laurent.philippot@inrae.fr

Author's adresses :

mathilde.jeanbille@inrae.fr, sana.romdhane@inrae.fr, marie-christine.breuil@inrae.fr, david.bru@inrae.fr, stefan.geisen@wur.nl, arnaud.mounier@inrae.fr, ayme.spor@inrae.fr , laurent.philippot@inrae.fr

Authorship

LP designed the study. DB, MJ, LP, SR, and AS were involved in the field work. MCB and MJ processed the samples. DB and MJ carried out the molecular analysis. MJ, SR, AS and AM analysed the data and performed the statistical analysis. MJ, SG, LP, SR, and AS discussed, interpreted and wrote the manuscript. All authors reviewed the manuscript.

Data availability statement

Raw sequences were deposited at the NCBI database under the BioProjects PRJNA1024461, PRJNA1024675 and PRJNA1024888 (https://www.ncbi.nlm.nih.gov/bioproject/). Source data and R scripts are available at https://doi.org/10.5281/zenodo.11072396

Running title: Microbial response to soil fauna exclusion

Keywords: interkingdom interactions, bacteria, fungi, protists, grassland soil, size-exclusion

This article is submitted as a *Letter* and contains :

- 149 words in abstract
- 4852 words in article
- 61 references
- 5 figures

ABSTRACT

Highly diverse and abundant organisms coexist in soils. However, the contribution of biotic interactions between soil organisms to microbial community assembly remains to be explored. Here, we assess the extent to which soil fauna can shape microbial community assembly using an exclusion experiment in a grassland field to sort soil biota based on body size. After one year, the exclusion of larger fauna favored phagotrophic protists, with increases up to 32% in their proportion compared to the no-mesh treatment. In contrast, members of the bacterial community and to a lesser extent of the fungal community were negatively impacted. Shifts in bacterial but not in fungal communities were best explained by the response of the protistan community to exclusion. Our findings provide empirical evidence of top-down control on the soil microbial communities and underline the importance of integrating higher trophic levels for a better understanding of the soil microbiome assembly.

INTRODUCTION

Soil biota encompass highly diverse organisms representing more than half of Earth's biodiversity (Anthony *et al.* 2023)(). Besides bacteria and fungi, which have traditionally been the most studied groups of soil-dwelling microorganisms, soil also serves as unique habitat for a broad range of protists, microfauna (e.g. nematodes, rotifers), mesofauna (eg. mites and collembolans) and macrofauna (eg. earthworms and insect larvae) (Potapov *et al.* 2022). Not only body size but also density of these organisms thriving in soil can span several orders of magnitude (Veresoglou *et al.* 2015, Coleman *et al.* 2024). A recent work showed that the community assembly of the smallest soil organisms was influenced by dispersal-based stochastic processes compared to larger ones, which are more structured by selection-based deterministic processes (Luan *et al.* 2020). It is recognized that inter-kingdom biotic interactions are commonplace in soil, resulting in an extraordinarily complex soil food web (Potapov *et al.* 2023; Scheu 2002). Understanding the importance of these interactions between soil fauna, fungi and prokaryotes is crucial for linking soil biodiversity and terrestrial ecosystem functioning (Bonkowski 2004; Crowther *et al.* 2015; Geisen *et al.* 2020). However, despite the key role of the soil bacteria and fungi in biogeochemical cycling (Falkowski *et al.* 2008), we know little about the contribution of biotic interactions between soil organisms to microbial community assembly.

Soil bacteria and fungi can be preyed upon by many soil organisms including protists, nematodes and collembolans (Potapov *et al.* 2022). For example, 75 % of the protistan soil community includes bacterial predators (Oliverio *et al.* 2020) and more than 129 species of bacterivorous nematodes have been identified (Martins *et al.* 2022). These microbial predators are themselves preyed by larger soil animals such as mites and tardigrades (Potapov *et al.* 2022). The addition of microbial predators in laboratory experiments revealed significant effects on fungal and bacterial communities

(Bell *et al.* 2010; Glücksman *et al.* 2010; Rosenberg *et al.* 2009), with preferential feeding on certain microbial species (Amacker *et al.* 2022; Asiloglu *et al.* 2021; Shu *et al.* 2021). Indirect interactions such as interference or exploitative competition are also numerous in terrestrial ecosystems (Neidig *et al.* 2010), although their impact remains elusive. Previous reductionist studies manipulating prey or predator communities have provided valuable insights into microbe-fauna interactions and feeding preferences of individual species (Bell *et al.* 2010; Karakoç *et al.* 2020; Saleem *et al.* 2012), but they often overlooked how these interactions are affected by larger organisms and by higher-order interactions. In contrast, observational studies of natural environments using correlation-based approaches for uncovering interactions between soil microbes are limited because correlations can emerge as a result of both species interactions and of environmental filtering (Faust 2021). As such, the relative importance of the different faunal groups in shaping the soil microbiome remains largely unresolved.

Here, we seek to determine the extent to which micro-, meso- and macro- fauna mediate the assembly of the soil microbiome. For this purpose, we used the large differences in body size between organisms to fractionate the soil community (Bradford *et al.* 2002; Briones 2014) and conducted an *in situ* exclusion experiment using microcosms with windows covered by various mesh sizes, for a differential sorting of the soil organisms. These exclusion microcosms containing sterile soil were buried in a grassland soil for up to 12 months and shifts in the soil biota were compared between size exclusion treatments during soil recolonization. We hypothesized that differential exclusion of soil fauna will lead to changes in community composition during soil recolonization therefore unraveling the importance of top-down interactions for microbial community assembly. Differential abundance analysis was used to identify the 18S rRNA and 16S rRNA OTUs exhibiting significant responses to exclusion treatments. We also inferred networks using the exclusion treatments as covariate to

distinguish the associations between soil organisms that were specifically related to the exclusion treatment from covariation patterns due to other mechanisms. Our results highlight the contribution of the soil fauna in shaping microbial community assembly with cascading effects across the food web and differential responses of protistan, bacterial and fungal communities, therefore further supporting the importance of top-down controls on microbial communities.

MATERIALS AND METHODS

Site description and design of the exclusion experiment

The field experiment was set up in a permanent grassland at the INRAE center, located in Dijon, France (47° 19' 01.7" N, 5° 04' 26.9" E). The soil properties were 33.8 % clay, 48.2 % silt, and 18 % sand, pH 6.31, and C and N content 39.98 and 3.12 $g.kg^{-1}$ dry soil, respectively. To quantify the importance of the micro- (< 100 µm), meso- (> 100 µm and < 2000 µm) and macro-fauna (>2000 µm) for soil microbial community assembly, we used exclusion microcosms consisting in 70 x 33 mm PVC pots with 6 windows (3 on the side, one on the bottom and one on the top, Fig. S1A), each covered and sealed with nylon membranes having different mesh sizes (i.e. 31, 50, 100, 250, 500, 1000 µm; Nitex®). The microcosms were filled with 4 mm sieved soil collected at the experimental field and then γ-sterilized (min 60 kGy, at Conservatome, Dagneux, France). On September 1st 2020, the exclusion microcosms were buried at a depth of c.a. 12 cm (Fig. S1B) following a complete randomized block design. The soil was drilled with a saw hole, and the topsoil from the saw hole was replaced over the microcosm after burial. Twelve exclusion cages per mesh size (n=12) were collected after 3 months (08/12/20, T1), 9 months (06/11/2021, T2) and 12 months (09/23/21, T3) for a total of 216 microcosms (6 mesh sizes x 3 sampling times x 12 replicates). Six control microcosms (n=6) with

windows not covered with mesh were collected at T3 only. Soil cores collected randomly from each block before microcosm burial (*i.e*. T0 original soil, 63 samples) were also used for subsequent analyses. After sampling, water content in each microcosm was determined by drying the soil for 24h at 105°C (Fig. S1). Additionally, precipitation and temperature data were retrieved from the nearest meteorological station (5.5 km away) (Fig. S1). Three microcosms from the 31 µm exclusion treatment that had visible holes larger than 1 mm at the harvest time were excluded from the following analysis.

DNA extraction and sequencing

The soil from each microcosm was thoroughly homogenized before DNA extraction. DNA was extracted from 285 samples (63 original soil samples and 222 microcosms) using the DNeasy PowerSoil-htp 96 well DNA isolation kit (Qiagen, France) according to the manufacturer's instructions. DNA concentration was estimated using Quant-IT™ dsDNA HS Assay kit (Invitrogen™, Carlsbad, CA, USA). To generate amplicons for sequencing, a 2-step PCR approach was used according to ref. (Berry *et al.* 2011). The V3-V4 hypervariable region of the 16S rRNA gene was amplified using the 341F (5'-CCTACGGGRSGCAGCAG-3') / 805R (5'-GACTACCAGGGTATCTAAT-3') primers. The V4 hypervariable region of the 18S rRNA gene was amplified with the EK-565F (5′-GCAGTTAAAAAGCTCGTAGT-3′) / 18S-EUK-1134-R–UnonMet (5′-TTTAAGTTTCAGCCTTGCG-5′) as well as with the M620F (5'-GCAGCCGCGGTAATTCC-3') / M1041R (5'-RCGRTCCAAGAATTTCACCTCT-3') primers, to study both metazoan and non-metazoan eukaryotes (Bower *et al.* 2004; Capra *et al.* 2016). The amplicon size was checked with 2 % agarose gel and the final PCR products were purified and their concentration normalized using the SequalPrep Normalization plate kit (Invitrogen™, Carlsbad, CA, USA). Sequencing was performed on

MiSeq (Illumina, 2 x 250 bp and 2 x 300 pb for 16S and 18S rRNA amplicons respectively) using the MiSeq reagent kit v2.

Amplicon sequence analysis

Demultiplexing and trimming of Illumina adaptors and barcodes was done with Illumina MiSeq Reporter software (version 2.5.1.3). Sequence data from soil samples were analysed using an in-house developed Python pipeline (available upon request). Briefly, 16S rRNA and 18S rRNA gene sequences were assembled using PEAR (Zhang *et al.* 2014) with default settings. Further quality checks were conducted using the QIIME pipeline (Caporaso *et al.* 2010) and short sequences were removed (< 400 bp for 16S rRNA gene and < 475 bp for 18S rRNA gene). Reference based and *de novo* chimera detection, as well as OTUs clustering were performed using VSEARCH (Rognes *et al.* 2016) and the adequate reference databases (SILVA 138 representative set of sequences (Quast *et al.* 2013) for 16S rRNA gene and the PR2 sequence database version 4.11.1 for 18S rRNA gene (Guillou *et al.* 2013). For 18S rRNA data, the two datasets, fully overlapping in the V4 region, were merged before OTUs clustering. The identity thresholds were set at 94 % for 16S based on replicate sequencing of a bacterial mock community (Romdhane *et al.* 2022) and 97 % for 18S. Representative sequences for each OTU were aligned using Infernal (Nawrocki & Eddy 2013) and phylogenetic trees were constructed using FastTree (Price *et al.* 2010). Taxonomy was assigned using UCLUST (Edgar 2010) and the SILVA database (138.1/2020) (Quast *et al.* 2013) for the 16S and 18S rRNA gene sequences, and the PR2 database (version 4.11.1) (Guillou *et al.* 2013) for the 18S rRNA sequences. 18S rRNA OTUs were assigned to Fungi when congruent PR2 and SILVA taxonomic assignations were found. 18S rRNA gene data was split into fungal, protistan and metazoan tables for further analysis. Trophic protist assignations were based on reference tables from refs. (Dumack *et al.* 2020; Ramond *et al.* 2018).

Statistical analysis

All statistical analyses were conducted using R statistical software version 4.2.1 (R Core Team 2018).

Alpha-diversity analyses

Following rarefaction with subsample sizes of 10,696, 1817 and 1690 for bacteria, fungi and non-fungal 18S rRNA OTUs respectively, observed richness was calculated using the vegan package version 2.5-7 (Oksanen *et al.* 2013). Effects of sampling time and exclusion treatment were assessed independently on alpha-diversity indices. Since normality and homoscedasticity of linear models residuals was not achieved, non-parametric Kruskal-Wallis test followed by post-hoc Dunn's test were performed using the package rstatix 0.7.0.

Beta-diversity analyses

Based on the whole datasets (singletons excluded), bayesian estimation of the sparse read counts using the CoDaSeq package version 0.99.6 (Gloor & Reid 2016) was computed before a centered log-ratio transformation with the zCompositions package version 1.3.4 (Palarea-Albaladejo & Martín-Fernández 2015), in order to account for compositionality of the data (Gloor et al. 2017). To assess the sources of variation (i.e. sampling time and exclusion treatment) in the Euclidean matrices of the centered log-ratio transformed bacterial, fungal, protistan and metazoan community data, we used principal component analysis and one-way permutational multivariate analysis of variance (PerMANOVA (McArdle & Anderson 2001)) with 10,000 permutations constrained by the block variable using the

182 'strata' option of the function adonis in the vegan package version 2.5-7 (Oksanen et al. 2013). For
183 each group, coordinates of control samples at T3 on the first and second axis of the principal
184 component analysis (PC1 and 2) were used to define the position of no-mesh control centroids (i.e., the
185 mean of the coordinates of control samples), and subsequently the distances of other sample positions
186 on PC1 and PC2 to these centroids. These distances to control centroids, referred as responses to
187 exclusion later on (accounting for the cumulated variance captured by the respective PCs), were then
188 used to perform stepwise multiple regressions, with the response to exclusion of each group as response
189 variable and other group responses as explanatory variables. Thus, these models aimed at inferring the
190 dependencies between the responses to exclusions of the bacterial, fungal, protistan and metazoan
191 communities. Best models were selected stepwisely using the Aikake Information Criterion (AIC) from
192 the MASS package version 7.3-58 (Venables & Ripley 2013), and model residuals checked for
193 normality and homoscedasticity.

194

195 *Assessment of community assembly processes*

196 The β-nearest taxon index (βNTI) was calculated according to Stegen et al. 2012, with 99 iterations and
197 weighted abundances using the Picante package version 1.8.2 (Kembel et al. 2010), in order to quantify
198 the turnover in phylogenetic composition. βNTI is the standard effect size between observed and null β-
199 mean nearest taxon distance (βMNTD). $|\beta NTI| > 2$ shows a significant deviation from the null βMNTD
200 distribution, thus indicating a dominance of deterministic processes, while $|\beta NTI| < 2$ indicates the
201 dominance of stochastic processes (Dini-Andreote et al. 2015). βNTI was quantified by pairwise
202 comparisons of communities from the same treatment at each sampling time. Because of skewed
203 distributions, Kruskal-Wallis tests followed by Dunn's test with Bonferroni corrections were used to
204 detect significant differences between times.

205

206 *Identification of differentially abundant OTUs in treatments*

207 Low-abundance OTUs were filtered out by keeping OTUs that (i) represented > 0.02 % of the
208 sequences across samples and (ii) were found in at least 60 % of one treatment replicates for each time
209 sampling time. This resulted in 416, 634 and 703 bacterial OTUs, 49, 66 and 72 fungal OTUs, 202,
210 215, and 215 protistan OTUs, and 2, 4, and 5 metazoan OTUs at T1, T2 and T3, respectively. We
211 referred to those OTUs with high abundances as "dominant" OTUs later on. To estimate differences in
212 relative abundances of the dominant OTUs between treatments, we used a generalized linear mixed
213 model (GLMM). Such model combines a generalized linear model, which allow to infer linear
214 regression from data that does not follow a Normal distribution as abundance data typically follow a
215 Poisson distribution, with a mixed model, containing both fixed (treatment effects) and random effects
216 (sampling effects). We considered that an OTU of abundance Y follows a Poisson law of parameter Λ
217 as $Y \sim P(\Lambda)$, in any replicates of any i treatment. Thus, we used the following model (Eq. 1):

218 $$log(\Lambda_{ij}) = o_{ij} + \mu + \alpha_i + Z_{ij}, Z_{ij}{}_{1 \le j \le 12} \text{ iid} \sim N(0, \sigma^2) (1)$$

219 where o is the offset for each sample calculated as the log of the sample read sum, α is the effect of the
220 exclusion treatment coded as a factor, and Z is the random sampling effect modeling the data
221 overdispersion. $i = \{1, \dots, 6\}$ represents the exclusion treatments for each microbial group (bacteria,
222 fungi or fauna), and $j = \{1, \dots, 12\}$ represents the replicates. The analysis was performed using the
223 glmer function of the lme4 package version 1.1-27 (Bates *et al.* 2014). Subsequently, we performed
224 multiple pairwise comparisons with the emmeans function of the emmeans package version 1.6.1
225 (Lenth 2018) for each OTU i) between all exclusion treatments and 1000 µm mesh size treatment for
226 T1, T2, T3 and ii) between all exclusion treatments and no-mesh control for T3. The p-values were then

adjusted using the false discovery rate (FDR) method (Benjamini & Hochberg 1995). Log2-fold changes were calculated as the ratios of the mean relative abundance in treatment to the mean relative abundance in control on a log2 scale. Only OTUs with FDR adjusted p-values below or equal to 0.05 and log2-fold change > 0.5 were considered as significantly affected by exclusion.

Inference of co-occurrence networks

Networks were constructed based on the dominant OTU count data (low-abundance OTUs filtered out) using samples from T3 including no-mesh control cages (n=78). Networks were inferred using a sparse multivariate Poisson log-normal (PLN) model with a latent Gaussian layer and an observed Poisson layer using the PLNmodels package version 1.0.1 (Chiquet *et al.* 2019). A specific normalization corresponding to the log-transformed number of reads in each sample was added as an offset in order to take into account the heterogeneity of sequencing depth within and between groups. For each sample set, we used one model without (null model, m0) and one model with the exclusion treatment (full model, m1) as a covariate to identify nodes and links specific to the mesh treatment. In any case, abiotic filtering was intrinsically limited by our approach since exclusion microcosms were filled with sterile soil, which was previously sieved and homogenized, before burying the microcosms in a 36 m^2 plot. All models included a block covariate to remove nodes and links related to the block effect. For each model, the best network was selected using a Stability Approach to Regularization Selection (StARS) (Liu *et al.* 2010), which performs a random subsampling of the input data to select a network with a very high stability of the selected edges (stability criteria set to 0.99). The network m0 – m1 was computed by substracting edges of the m1 to edges of the m0 model.

RESULTS

Colonization dynamics of the exclusion microcosms. The colonization dynamic of the exclusion microcosms was assessed by DNA metabarcoding targeting the bacterial, fungal, protistan and metazoan communities at 3 months (T1), 9 months (T2) and 12 months (T3) (Fig. S2). We found differential colonization dynamics between organisms, with the sampling time significantly affecting the diversity and structure of the bacterial, fungal, protistan and metazoan communities (Figs S3 and S4). Three months after burying the soil microcosms, the richness of all studied soil communities was significantly lower than at T0, with a reduction ranging from 34% to 58 % (Fig. S3). After 9 and 12 months (T2 and T3, respectively), we observed that the richness increased compared to T1 but only the diversity of the bacterial community reached the diversity observed in the natural soil at T0 (Fig. S3, Dunn's test $p < 0.001$). Similarly, the bacterial, fungal, protistan and metazoan community compositions also differed significantly across sampling time (Fig. S4), with a higher variance in community structure explained by the sampling time for bacteria (29 %, $p < 0.001$) followed by fungi (22 %, $p < 0.001$), protists (18 %, $p < 0.001$), and metazoa (14 %, $p < 0.001$). The higher differences between T1 and T3 (16 % for bacteria, 11 % for fungi, 6 % for protists, and 7 % for metazoans PerMANOVA $p < 0.001$) than between T1 and T2 (10 % for bacteria, 6 % for fungi, 5 % for protists, and 6 % for metazoans, PerMANOVA $p < 0.001$), suggest that the colonization process slowdown with time. We also calculated the βNTI to evaluate the relative influences of distinct community assembly processes during soil colonization (Fig S3). The same patterns of βNTI were observed for most communities, with the largest changes occurring at T1, and βNTI values at T3 that were either closer to or not different from those at T0. Notably, a greater influence of stochasticity was observed for the bacteria at T1 during the initial phase of soil colonization while bacterial community assembly was dominated by deterministic processes at T0.

Shifts in community diversity and composition in response to exclusion

After 12 months, we observed significant effects of the exclusion treatments on diversity but to different extent depending on the organism group. The diversity of the bacterial community was weakly impacted by exclusion in 31 µm exclusion treatment only compared to the no-mesh control (Fig. 1A, Dunn's test, $p < 0.001$). Larger differences in protistan diversity were also observed between the exclusion treatments and the no-mesh control with a decrease of up to 26 % in species richness, respectively (Fig. 1A, Dunn's test, $p < 0.001$). A stronger response to exclusion was observed when the mesh size was lower than 1000 µm and 100 µm for the fungal and metazoan community, respectively (Fig. 1A, Dunn's test, $p < 0.001$). Exclusion also impacted the composition of the soil communities with significant effects at all sampling dates (Fig. S5). At T3 including the no-mesh control, 17 %, 14 %, 15 % and 12 % of variation in the bacterial, fungal, protistan and metazoan communities, respectively, were related to the mesh size (Fig 1B, PerMANOVA, $p < 0.001$). However, significant differences were mostly observed in the microcosms covered with a mesh size of 500 µm or larger (Table S1). We also calculated the distances between the exclusion treatments and the no-mesh control based on ordinations of centered log-ratio transformed community data **(**Fig 1B). By doing so, we measured the responses to exclusion, captured as a portion of the amount of variance explained by the ordinations, and then inferred the relationships between the responses to exclusion of the bacterial, fungal, protistan and metazoan communities using stepwise multiple regressions. Our data revealed that the response of the metazoan community significantly explained 58 % of the variance of that of the protistan community to exclusion (Fig 1C, $p < 0.05$). The bacterial response also had a significant but weaker importance for the protistan response with only 18 % of the variance explained. In return, 47 % and 28 % of variation in the bacterial response were explained by the protistan and fungal responses, respectively. Reciprocally, the fungal response to exclusion was explained by the bacterial response

296 only (Fig 1C). The explained variance in the metazoan response to the exclusion was the lowest and
297 driven by the protistan response (28 %).
298
299 **Identification of the exclusion-impacted OTUs**
300 To further identify OTUs that were affected by the mesh size, we used a generalized linear mixed
301 model accounting for the inherent compositional nature of the data to estimate significant differences in
302 the relative abundances of dominant OTUs between treatments for each sampling time. In accordance
303 with the observed shifts in community composition with time, the number of dominant OTUs
304 exhibiting significant changes in relative abundance was higher at T2 and T3 than at T1 (Figs. S6 to S8,
305 Table S2, fdr-adjusted $p < 0.05$). Regardless of the sampling time, the response to exclusion treatments
306 was asymmetrical with bacterial and fungal OTUs exhibiting a negative rather than a positive response,
307 whereas the opposite was observed for the protistan OTUs (Fig 2A, Fig. S6). Thus, using the no-mesh
308 control as reference at T3, we found that OTUs with significantly decreasing relative abundances
309 across treatments represented 63 % and 71 % of the affected bacterial and fungal OTUs respectively,
310 while 78 % of the affected protistan OTUs showed an increase in relative abundance in the exclusion
311 treatments (Table S2; fdr-adjusted $p < 0.05$). Overall, 46, 35 and 25 % of the dominant bacterial, fungal
312 and protistan OTUs were significantly affected by the exclusion treatments compared to the no-mesh
313 control at T3. Phagotrophic protists belonging to Cercozoa, Ciliophora and Stramenopiles lineages
314 represented 89 % of the protistan OTUs positively impacted by exclusion treatments (Fig. 3).
315 Conversely, more than half of the negatively impacted fungal OTUs belonged to the Ascomycota (Fig.
316 3). Alphaproteobacteria and Gammaproteobacteria represented 49 % of bacterial OTUs with positive
317 response to exclusion treatment, while 68 % of those with a negative response belonged to
318 Actinobacteria, Verrucomicrobia, Acidobacteria and Bacteroidetes (Fig. 4). Whatever the community,
319 the magnitude of changes in relative abundances (*i.e.* absolute log2-fold changes) and the percentage of

impacted OTUs were the smallest in the 1000 µm exclusion treatment (Figs. 2 to 4, Dunn's test, $p <$ 0.001). At the most 5 metazoan OTUs were affected by size exclusion at T3 including no-mesh controls (Table S2).

Exclusion-specific co-occurrence networks

In order to evaluate how the exclusion treatments affected bacterial, fungal, protistan and metazoan co-occurrences, we inferred inter-kingdom networks without covariate (m0) and with the exclusion treatment as a qualitative covariate (m1). We then identified the nodes and edges that were statistically related to the exclusion treatments exclusively (*i.e.* differentially identified between m0 and m1 models). After12 months, we found that the most abundant interkingdom edges were between bacteria and protists (327) or between fungi and bacteria (266) (Fig. 5). Interestingly, negative edges connecting cercozoans to Bacteroidetes represented 65 % of the negative edges between bacteria and protists and 90 % of the negative edges between cercozoans and bacteria (Fig. 5B and C). Edges between fungi and protists represented only 5.4 % of the total network edges while edges involving metazoans represented less than 1 % of the network (Fig. 5A).

DISCUSSION

To assess the importance of the soil fauna in microbial community assembly, we buried sterile soil microcosms covered with mesh sizes ranging between 31 and 1000 µm to prevent colonization by soil organisms according to their body size. One year after microcosm burial in a grassland field, we observed a decrease in faunal diversity along with shifts in faunal community composition in the exclusion treatments compared to the no-mesh control. However, in contrast to our initial expectations

based on the large variations in body size among the studied organisms, weak to no differences were found between microcosms with mesh size ranging from 31 to than 500 µm. This could be due to an underestimation of the effect of the exclusion treatments on the soil fauna, given the lower probability of retrieving organisms with low abundance in soil, such as members of the mesofauna and macrofauna (Capra *et al.* 2016). In addition, the exclusion of larger organisms may also have limited the dispersal capacities of other members of the soil communities. Thus, phoresy, which is a dispersal strategy in which an organism attaches to an animal for transportation, is common in mites (Seeman & Walter 2023). Similarly, phoresy on mites or isopods has been shown to represent mechanisms of dispersal for nematodes and protists (Bharti *et al.* 2020; Eng *et al.* 2005). Nevertheless, multiple regression analysis showed that 58 % of the variation in the response of the protistan community to exclusion at T3 was explained by that of metazoa. In return, the magnitude of the response of the protists was the main driver influencing that of the bacterial community, which suggests cascading effects of the soil fauna on microbial community assembly. However, note that the percentage of variance captured by the PCA was at the most 19.4%. By using a generalized linear mixed model for differential abundance analysis, we identified among the dominant taxa those responding significantly to the exclusion treatments. The affected protistan OTUs exhibited an increase rather than a decrease in relative abundance in the exclusion treatments. The most common soil protists have an average body size between 8 and 21 µm (Luan *et al.* 2020) and, accordingly protists positively affected by exclusion were gradually more numerous with decreasing mesh size until 31 µm. These affected protistan OTUs mostly belonged to the phagotrophic protists, resulting in an increase of the general proportion of phagotrophic protists of up to 32% compared to the no-mesh control. This suggests a competitive advantage of phagotrophic protists, either directly or indirectly, when larger fauna was increasingly excluded. Thus, protists are preyed upon by larger organisms like Oribatids or Collembola in grassland soils (Crotty *et al.* 2012), and the exclusion treatments may have provided a shelter allowing protists present in the exclusion

366 microcosms to thrive. Accordingly, Erktan *et al*. (Erktan *et al.* 2020) suggested that soil pores of
367 contrasting sizes could provide refuges, leading to segregation between prey and predators, therefore
368 affecting top-down controls. Alternatively, the exclusion of competitors also feeding on bacteria such as
369 microarthropods (e.g. collembolans and oribatids) and nematodes (Thakur & Geisen 2019) could have
370 left a broader niche and larger food source to the phagotrophic protists, even though diet preference
371 between bacterivores are still unclear. The positive response of phagotrophic protists to exclusion was
372 mirrored by a decrease in relative abundance of the dominant bacterial and fungal OTUs, among which
373 70 % and 80 % of the OTUs, respectively, were negatively and significantly affected by the exclusion
374 treatments. Overall, the OTUs affected by the exclusion treatments accounted for 46 %, 35 % and 27 %
375 of the dominant bacterial fungal and protistan OTUs, respectively, which underlines the importance of
376 the interplay between different trophic levels in soil and top-down effects on the soil microbiome.

377 Our co-occurrence network approach provided additional information on which associations
378 between the soil organisms were directly related to the exclusion treatments. Thus, the inference of
379 networks using the exclusion treatments as covariate allowed us to exclude co-variation caused by
380 abiotic filtering and to identify co-variations specifically induced by exclusion (Chiquet *et al.* 2021).
381 Negative edges specifically induced by exclusion were numerous between cercozoans and bacteria with
382 90 % of these edges comprising Bacteroidetes. Interestingly, the soil bacterial community was
383 dominated by Proteobacteria (59 %), while Bacteroidetes represented only 12 %. Thus, our results
384 suggest that prey switching, where the predator preferentially consumes the most abundant type of prey
385 as it can be observed in simplified systems with a single prey, is not the feeding strategy of cercozoans.
386 Instead, our field exclusion experiment supports previous studies suggesting that Bacteroidetes are
387 preferred prey sources for protists (Asiloglu *et al.* 2021; Flues *et al.* 2017). In contrast, the number of
388 edges connecting protists and fungi was much smaller, which echoes the absence of a significant

relationship between the responses of the fungal and protistan community to the exclusion treatments. However, the high number of edges between bacteria and fungi, as well as the high percentage of variance in the response of the fungal community to exclusion explained by the bacterial communities (50 %), suggest that fungal community assembly is mostly influenced by bacteria (Bahram *et al.* 2018).

In conclusion, our experimental approach showed that exclusion of the soil fauna according to body size led to cascading effects through the food web with both direct and indirect interactions. In particular, exclusion of larger soil fauna positively impacted phagotrophic protists with subsequent effects on microbial community composition. Overall, our findings provide unique information on the driving factors governing soil microbiome assembly *in situ* by unveiling the contribution of the top-down control by soil protists on the bacterial community composition with indirect effects on the fungal community. Since our experimental approach aimed at controlling environmental filtering and therefore resulted in a low variation in the resource level, future work is needed to assess the relative contribution of top-down and bottom-up processes as well as of their interactions in shaping soil microbial communities.

Conflict of interest statement

The authors declare no competing interests

Funding

This research was funded by the ISITE-UBFC senior fellowship, grant RA19016.AEC.IS.

Figure and table legends

Figure 1. Effect of the mesh exclusion treatment on bacterial, fungal, protistan and metazoan communities. A) Bacterial, fungal, protistan and metazoan observed richness across exclusion treatments at T3 (n=9 for treatment 31 µm, n=12 for treatments 50 to 1000 µm and n=6 for no-mesh). Boxes show the inter-quartile range between the 1st and 3rd quartiles, with median indicated by the line and whiskers indicate the maximum and minimum of the inter-quartile range. Different lowercase letters indicates significant difference within each panel ($p < 0.05$) determined with one-way Kruskal-Wallis test and post-hoc Dunn's test. B) Principal component ordinations of bacterial, fungal, protistan and metazoan communities at T3 across exclusion treatments and no-mesh controls, based on Euclidean distances of centered log-ratio transformed OTU abundances. The effects of exclusion treatment for each organism group and sampling time were tested with PerMANOVA (** $p < 0.01$, *** $p < 0.001$) and are displayed above each ordination. Ellipses represent 95 % confidence level around each treatment centroid. C) Significant linear relationships (ANOVA, $p < 0.05$) between the responses to exclusion of the bacterial, fungal, protistan and metazoan communities, based on multiple regression models. Community response to exclusion was quantified by the beta-diversity distances to the no-mesh control centroid. The proportion of variance explained by the best predictors, as determined using stepwise AIC, is shown for each group.

Figure 2. Proportion and response magnitude of the bacterial, fungal and protistan OTUs affected by the mesh exclusion treatment at T3 as identified using the GLM model. A) Proportion of dominant OTUs with significantly increasing (blue) or decreasing (red) relative abundances in each exclusion treatment compared to no-mesh controls (fdr-adjusted $p < 0.05$). B) Log2-fold changes in the relative abundances of significantly affected OTUs in each exclusion treatment, relative to the no-mesh

control. Log2-fold change medians are represented by black lines. Only 5 metazoan OTUs were affected by exclusion treatments, and therefore are not shown.

Figure 3. Taxonomic assignment and distribution of significantly impacted protistan, metazoan and fungal OTUs by the mesh exclusion treatment at T3. Heatmap showing the log2-fold changes in the relative abundances of significantly increasing (blue shades) and decreasing (red shades) OTUs for each exclusion treatment, relative to the no-mesh control. The outer ring shows the trophic modes based on taxonomic assignments, where bacterivore, myzocytotic, omnivore and eukaryvore are defined here as finer trophic assignations within phagotrophs. The OTU taxonomy is indicated by different colors on the innermost ring.

Figure 4 Taxonomic assignment and distribution of significantly impacted bacterial OTUs by the mesh exclusion treatment at T3. Heatmap showing the log2-fold changes in the relative abundances of significantly increasing (blue shades) and decreasing (red shades) OTUs for each exclusion treatment, as compared to the no-mesh control. The OTU taxonomy is indicated by different colors on the innermost ring.

Figure 5. Network edges specifically induced by exclusion. A) Number of positive and negative edges occurring between the different groups and statistically related to the exclusion treatment in the m0 – m1 network. B) Chord diagram showing the distribution of negative edges between protistan and metazoan (blues shades) and bacterial nodes (orange shades). The node taxonomy is represented at the

454 phylum or class level. C) Number of positive and negative edges of the m0 – m1 network involving
455 Cercozoa and bacteria, sorted by phylum or class.

456

457 **REFERENCES**

Amacker, N., Gao, Z., Hu, J., Jousset, A.L.C., Kowalchuk, G.A. & Geisen, S. (2022). Protist feeding patterns and growth rate are related to their predatory impacts on soil bacterial communities. *FEMS Microbiology Ecology*, 98, fiac057.

Anthony, M.A., Bender, S.F. & van der Heijden, M.G.A. (2023). Enumerating soil biodiversity. *Proceedings of the National Academy of Sciences*, 120, e2304663120.

Asiloglu, R., Kenya, K., Samuel, S.O., Sevilir, B., Murase, J., Suzuki, K., *et al.* (2021). Top-down effects of protists are greater than bottom-up effects of fertilisers on the formation of bacterial communities in a paddy field soil. *Soil Biology and Biochemistry*, 156, 108186.

Bahram, M., Hildebrand, F., Forslund, S.K., Anderson, J.L., Soudzilovskaia, N.A., Bodegom, P.M., *et al.* (2018). Structure and function of the global topsoil microbiome. *Nature*, 560, 233–237.

Bates, D., Mächler, M., Bolker, B. & Walker, S. (2014). Fitting Linear Mixed-Effects Models using lme4. *arXiv:1406.5823 [stat]*.

Bell, T., Bonsall, M.B., Buckling, A., Whiteley, A.S., Goodall, T. & Griffiths, R.I. (2010). Protists have divergent effects on bacterial diversity along a productivity gradient. *Biology Letters*, 6, 639–642.

Benjamini, Y. & Hochberg, Y. (1995). Controlling the False Discovery Rate: A Practical and Powerful Approach to Multiple Testing. *Journal of the Royal Statistical Society: Series B (Methodological)*, 57, 289–300.

Berry, D., Mahfoudh, K.B., Wagner, M. & Loy, A. (2011). Barcoded Primers Used in Multiplex Amplicon Pyrosequencing Bias Amplification. *Appl. Environ. Microbiol.*, 77, 7846–7849.

Bharti, D., Kumar, S., Laterza, A. & Chandra, K. (2020). Dispersal of ciliated protist cysts: mutualism and phoresy on mites. *Ecology*, 101, 1–3.

Bonkowski, M. (2004). Protozoa and plant growth: the microbial loop in soil revisited. *New Phytologist*, 162, 617–631.

Bower, S.M., Carnegie, R.B., Goh, B., Jones, S.R.M., Lowe, G.J. & Mak, M.W.S. (2004). Preferential PCR Amplification of Parasitic Protistan Small Subunit rDNA from Metazoan Tissues. *Journal of Eukaryotic Microbiology*, 51, 325–332.

Bradford, M.A., Jones, T.H., Bardgett, R.D., Black, H.I.J., Boag, B., Bonkowski, M., *et al.* (2002). Impacts of Soil Faunal Community Composition on Model Grassland Ecosystems. *Science*, 298, 615–618.

Briones, M.J.I. (2014). Soil fauna and soil functions: a jigsaw puzzle. *Frontiers in Environmental Science*, 2, 7.

Caporaso, J.G., Kuczynski, J., Stombaugh, J., Bittinger, K., Bushman, F.D., Costello, E.K., *et al.* (2010). QIIME allows analysis of high-throughput community sequencing data. *Nat Methods*, 7, 335–336.

Capra, E., Giannico, R., Montagna, M., Turri, F., Cremonesi, P., Strozzi, F., *et al.* (2016). A new primer set for DNA metabarcoding of soil Metazoa. *European Journal of Soil Biology*, 77, 53–59.

Chiquet, J., Mariadassou, M. & Robin, S. (2021). The Poisson-Lognormal Model as a Versatile Framework for the Joint Analysis of Species Abundances. *Frontiers in Ecology and Evolution*, 9.

Chiquet, J., Robin, S. & Mariadassou, M. (2019). Variational Inference for sparse network reconstruction from count data. In: *International Conference on Machine Learning*. Presented at the International Conference on Machine Learning, PMLR, pp. 1162–1171.

Coleman, D.C., Geisen, S. & Wall, D.H. (2024). Chapter 5 - Soil fauna: occurrence, biodiversity, and roles in ecosystem function. In: *Soil Microbiology, Ecology and Biochemistry (Fifth Edition)* (eds. Paul, E.A. & Frey, S.D.). Elsevier, pp. 131–159.

Crotty, F.V., Adl, S.M., Blackshaw, R.P. & Murray, P.J. (2012). Protozoan Pulses Unveil Their Pivotal Position Within the Soil Food Web. *Microb Ecol*, 63, 905–918.

Crowther, T.W., Thomas, S.M., Maynard, D.S., Baldrian, P., Covey, K., Frey, S.D., *et al.* (2015). Biotic interactions mediate soil microbial feedbacks to climate change. *Proceedings of the National Academy of Sciences*, 112, 7033–7038.

Dini-Andreote, F., Stegen, J.C., van Elsas, J.D. & Salles, J.F. (2015). Disentangling mechanisms that mediate the balance between stochastic and deterministic processes in microbial succession. *Proceedings of the National Academy of Sciences*, 112, E1326–E1332.

Dumack, K., Fiore-Donno, A.M., Bass, D. & Bonkowski, M. (2020). Making sense of environmental sequencing data: Ecologically important functional traits of the protistan groups Cercozoa and Endomyxa (Rhizaria). *Molecular Ecology Resources*, 20, 398–403.

Edgar, R.C. (2010). Search and clustering orders of magnitude faster than BLAST. *Bioinformatics*, 26, 2460–2461.

Eng, M.S., Preisser, E.L. & Strong, D.R. (2005). Phoresy of the entomopathogenic nematode Heterorhabditis marelatus by a non-host organism, the isopod Porcellio scaber. *Journal of Invertebrate Pathology*, 88, 173–176.

Erktan, A., Or, D. & Scheu, S. (2020). The physical structure of soil: Determinant and consequence of trophic interactions. *Soil Biology and Biochemistry*, 148, 107876.

Falkowski, P.G., Fenchel, T. & Delong, E.F. (2008). The Microbial Engines That Drive Earth's Biogeochemical Cycles. *Science*, 320, 1034–1039.

Faust, K. (2021). Open challenges for microbial network construction and analysis. *ISME J*, 15, 3111–3118.

Flues, S., Bass, D. & Bonkowski, M. (2017). Grazing of leaf-associated Cercomonads (Protists: Rhizaria: Cercozoa) structures bacterial community composition and function. *Environmental Microbiology*, 19, 3297–3309.

Geisen, S.A., Lara, E., Mitchell, E. a. D., Völcker, E. & Krashevska, V. (2020). Soil protist life matters! *Soil Organisms*, 92, 189–196.

Gloor, G.B., Macklaim, J.M., Pawlowsky-Glahn, V. & Egozcue, J.J. (2017). Microbiome Datasets Are Compositional: And This Is Not Optional. *Front. Microbiol.*, 8.

Gloor, G.B. & Reid, G. (2016). Compositional analysis: a valid approach to analyze microbiome high-throughput sequencing data. *Can. J. Microbiol.*, 62, 692–703.

Glücksman, E., Bell, T., Griffiths, R.I. & Bass, D. (2010). Closely related protist strains have different grazing impacts on natural bacterial communities. *Environmental Microbiology*, 12, 3105–3113.

Guillou, L., Bachar, D., Audic, S., Bass, D., Berney, C., Bittner, L., *et al.* (2013). The Protist Ribosomal Reference database (PR2): a catalog of unicellular eukaryote Small Sub-Unit rRNA sequences with curated taxonomy. *Nucleic Acids Research*, 41, D597–D604.

Karakoç, C., Clark, A.T. & Chatzinotas, A. (2020). Diversity and coexistence are influenced by time-dependent species interactions in a predator–prey system. *Ecol Lett*, 23, 983–993.

Kembel, S.W., Cowan, P.D., Helmus, M.R., Cornwell, W.K., Morlon, H., Ackerly, D.D., *et al.* (2010). Picante: R tools for integrating phylogenies and ecology. *Bioinformatics*, 26, 1463–1464.

Lenth, R. (2018). Emmeans: Estimated marginal means, aka least-squares means.

Liu, H., Roeder, K. & Wasserman, L. (2010). Stability Approach to Regularization Selection (StARS) for High Dimensional Graphical Models. *Adv Neural Inf Process Syst*, 24, 1432–1440.

Luan, L., Jiang, Y., Cheng, M., Dini-Andreote, F., Sui, Y., Xu, Q., *et al.* (2020). Organism body size structures the soil microbial and nematode community assembly at a continental and global scale. *Nat Commun*, 11, 6406.

Martins, S.J., Taerum, S.J., Triplett, L., Emerson, J.B., Zasada, I., de Toledo, B.F., *et al.* (2022). Predators of Soil Bacteria in Plant and Human Health. *Phytobiomes Journal*, 6, 184–200.

McArdle, B.H. & Anderson, M.J. (2001). Fitting multivariate models to community data: a comment on distance-based redundancy analysis. *Ecology*, 82, 290–297.

Nawrocki, E.P. & Eddy, S.R. (2013). Infernal 1.1: 100-fold faster RNA homology searches. *Bioinformatics*, 29, 2933–2935.

Neidig, N., Jousset, A., Nunes, F., Bonkowski, M., Paul, R.J. & Scheu, S. (2010). Interference between bacterial feeding nematodes and amoebae relies on innate and inducible mutual toxicity. *Functional Ecology*, 24, 1133–1138.

Oksanen, J., Blanchet, F.G., Kindt, R., Legendre, P., Minchin, P.R., O'Hara, R.B., *et al.* (2013). Package 'vegan.'

Palarea-Albaladejo, J. & Martín-Fernández, J.A. (2015). zCompositions — R package for multivariate imputation of left-censored data under a compositional approach. *Chemometrics and Intelligent Laboratory Systems*, 143, 85–96.

Potapov, A., Lindo, Z., Buchkowski, R. & Geisen, S. (2023). Multiple dimensions of soil food-web research: History and prospects. *European Journal of Soil Biology*, 117, 103494.

Potapov, A.M., Beaulieu, F., Birkhofer, K., Bluhm, S.L., Degtyarev, M.I., Devetter, M., *et al.* (2022). Feeding habits and multifunctional classification of soil-associated consumers from protists to vertebrates. *Biological Reviews*, 97, 1057–1117.

Price, M.N., Dehal, P.S. & Arkin, A.P. (2010). FastTree 2 – Approximately Maximum-Likelihood Trees for Large Alignments. *PLOS ONE*, 5, e9490.

Quast, C., Pruesse, E., Yilmaz, P., Gerken, J., Schweer, T., Yarza, P., *et al.* (2013). The SILVA ribosomal RNA gene database project: improved data processing and web-based tools. *Nucl. Acids Res.*, 41, D590–D596.

R Core Team. (2018). R: A language and environment for statistical computing. R Foundation for Statistical Computing, Vienna, Austria.

Ramond, P., Siano, R. & Sourisseau, M. (2018). Functional traits of marine protists.

Rognes, T., Flouri, T., Nichols, B., Quince, C. & Mahé, F. (2016). VSEARCH: a versatile open source tool for metagenomics. *PeerJ*, 4, e2584.

Romdhane, S., Spor, A., Aubert, J., Bru, D., Breuil, M.-C., Hallin, S., *et al.* (2022). Unraveling negative biotic interactions determining soil microbial community assembly and functioning. *ISME J*, 16, 296–306.

Rosenberg, K., Bertaux, J., Krome, K., Hartmann, A., Scheu, S. & Bonkowski, M. (2009). Soil amoebae rapidly change bacterial community composition in the rhizosphere of Arabidopsis thaliana. *ISME J*, 3, 675–684.

Saleem, M., Fetzer, I., Dormann, C.F., Harms, H. & Chatzinotas, A. (2012). Predator richness increases the effect of prey diversity on prey yield. *Nat Commun*, 3, 1305.

Scheu, S. (2002). The soil food web: structure and perspectives. *European Journal of Soil Biology*, 38, 11–20.

Seeman, O.D. & Walter, D.E. (2023). Phoresy and Mites: More Than Just a Free Ride. *Annu. Rev. Entomol.*, 68, 69–88.

Shu, L., He, Z., Guan, X., Yang, X., Tian, Y., Zhang, S., *et al.* (2021). A dormant amoeba species can selectively sense and predate on different soil bacteria. *Functional Ecology*, 35, 1708–1721.

Stegen, J.C., Lin, X., Konopka, A.E. & Fredrickson, J.K. (2012). Stochastic and deterministic assembly processes in subsurface microbial communities. *ISME J*, 6, 1653–1664.

Thakur, M.P. & Geisen, S. (2019). Trophic Regulations of the Soil Microbiome. *Trends in Microbiology*, 27, 771–780.

Venables, W.N. & Ripley, B.D. (2013). *Modern applied statistics with S-PLUS*. Springer Science & Business Media.

Veresoglou, S.D., Halley, J.M. & Rillig, M.C. (2015). Extinction risk of soil biota. *Nat Commun*, 6, 8862.

Zhang, J., Kobert, K., Flouri, T. & Stamatakis, A. (2014). PEAR: a fast and accurate Illumina Paired-End reAd mergeR. *Bioinformatics*, 30, 614–620.

A

Bacteria

Fungi

Protists

Metazoa

Observed richness

Bacteria: a ab ab ab ab ab b

Fungi: a a ab a a bc c

Protists: ab ac ab abc ab b c

Metazoa: a a ab ab ab ab b

31 50 100 250 500 1000 no-mesh

B

F = 2.3, R² = 17 %***

F = 1.8, R² = 14 %***

F = 1.9, R² = 15 %***

F = 1.5, R² = 12 %***

PC2: .7 % explained variance

PC2: 7.8 % explained variance

PC2: 6.7 % explained variance

PC2: 8.2 % explained variance

PC1: 12.4 % explained variance

PC1: 8.7 % explained variance

PC1: 8.9 % explained variance

PC1: 8.9 % explained variance

Mesh size (µm) 31 50 100 250 500 1000 no-mesh

C

Response variable (distance to no-mesh)

Bacteria 47 28

Fungi 50

Protists 58 18

Metazoa 28

Explained variance

Bacteria

Fungi

Metazoa

Protists

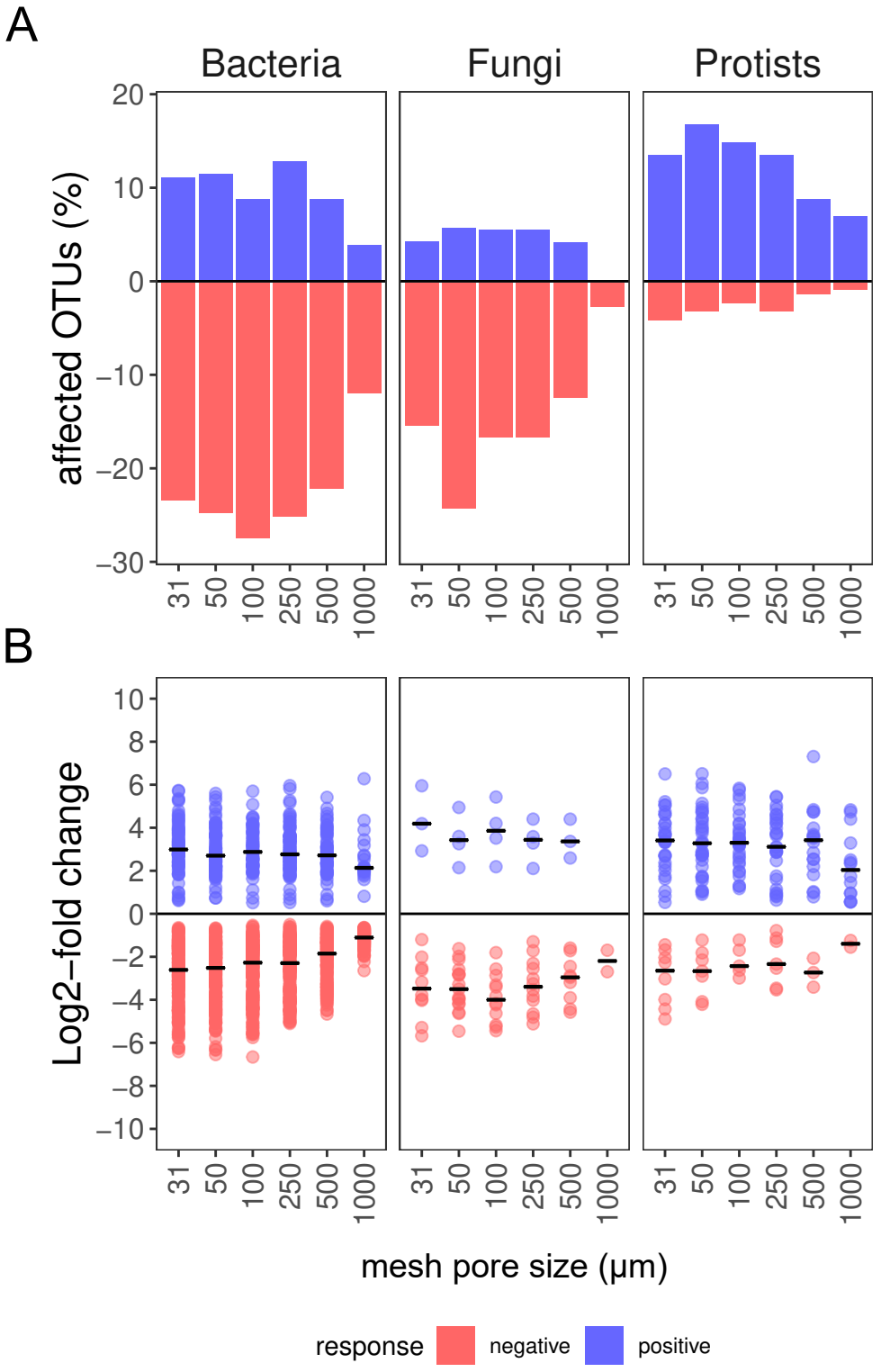
A
Bacteria
Fungi
Protists
affected OTUs (%)
20
10
0
−10
−20
−30
31
50
100
250
500
1000
B
Log2−fold change
10
8
6
4
2
0
−2
−4
−6
−8
−10
mesh pore size (μm)
response
negative
positive

Taxonomy

Protists

- Cercozoa
- Telonema
- Stramenopiles
- Choanoflagellida
- Apusozoa
- Amoebozoa
- Ciliophora
- Unclassified

Metazoa

- Nematoda
- Annelida

Fungi

- Ascomycota
- Basidiomycota
- Chytridiomycota
- Mucuromycota

Log2 Fold Change

-9 -7 -5 -3 -1 0 1 3 5 7 9

Trophic mode

- Phagotroph
  - Bacterivore
  - Myzocytotic
  - Omnivore
  - Eukaryvore
- Osmotroph
- Saprotroph
- Symbiotroph
- Endoparasite
- Parasite
- Unclassified

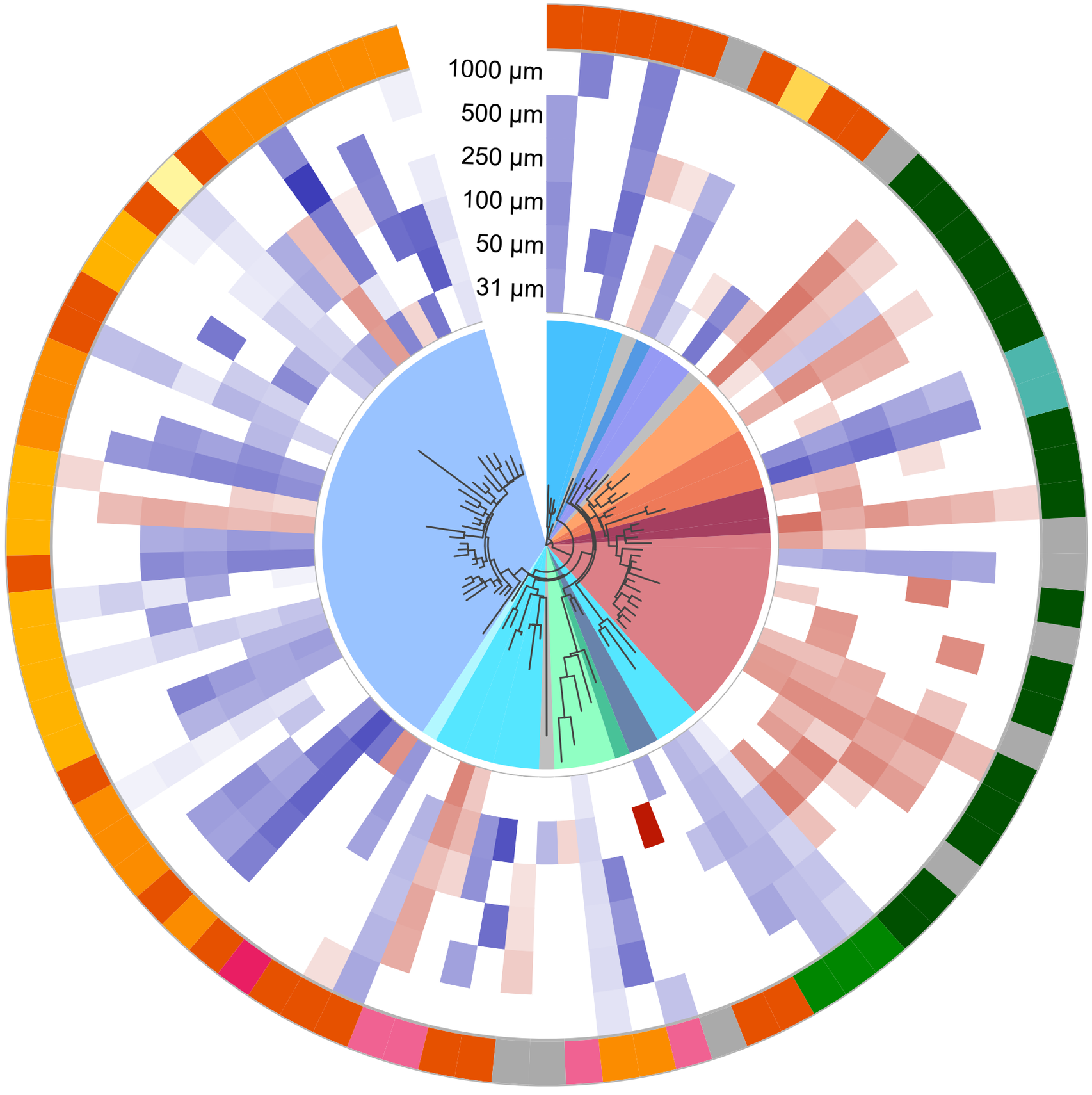

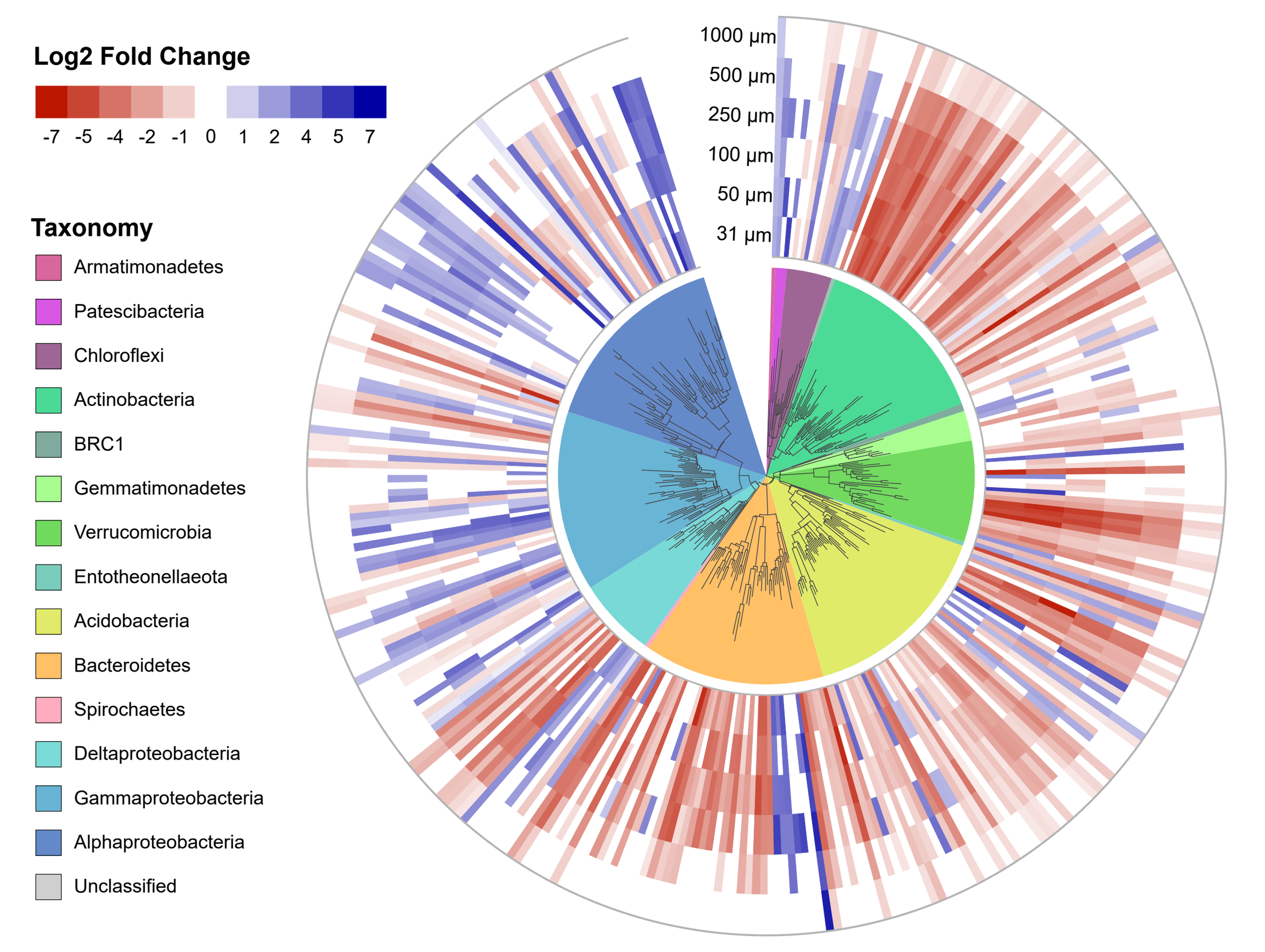
Log2 Fold Change
-7 -5 -4 -2 -1 0 1 2 4 5 7
Taxonomy
Armatimonadetes
Patescibacteria
Chloroflexi
Actinobacteria
BRC1
Gemmatimonadetes
Verrucomicrobia
Entotheonellaeota
Acidobacteria
Bacteroidetes
Spirochaetes
Deltaproteobacteria
Gammaproteobacteria
Alphaproteobacteria
Unclassified
1000 µm
500 µm
250 µm
100 µm
50 µm
31 µm

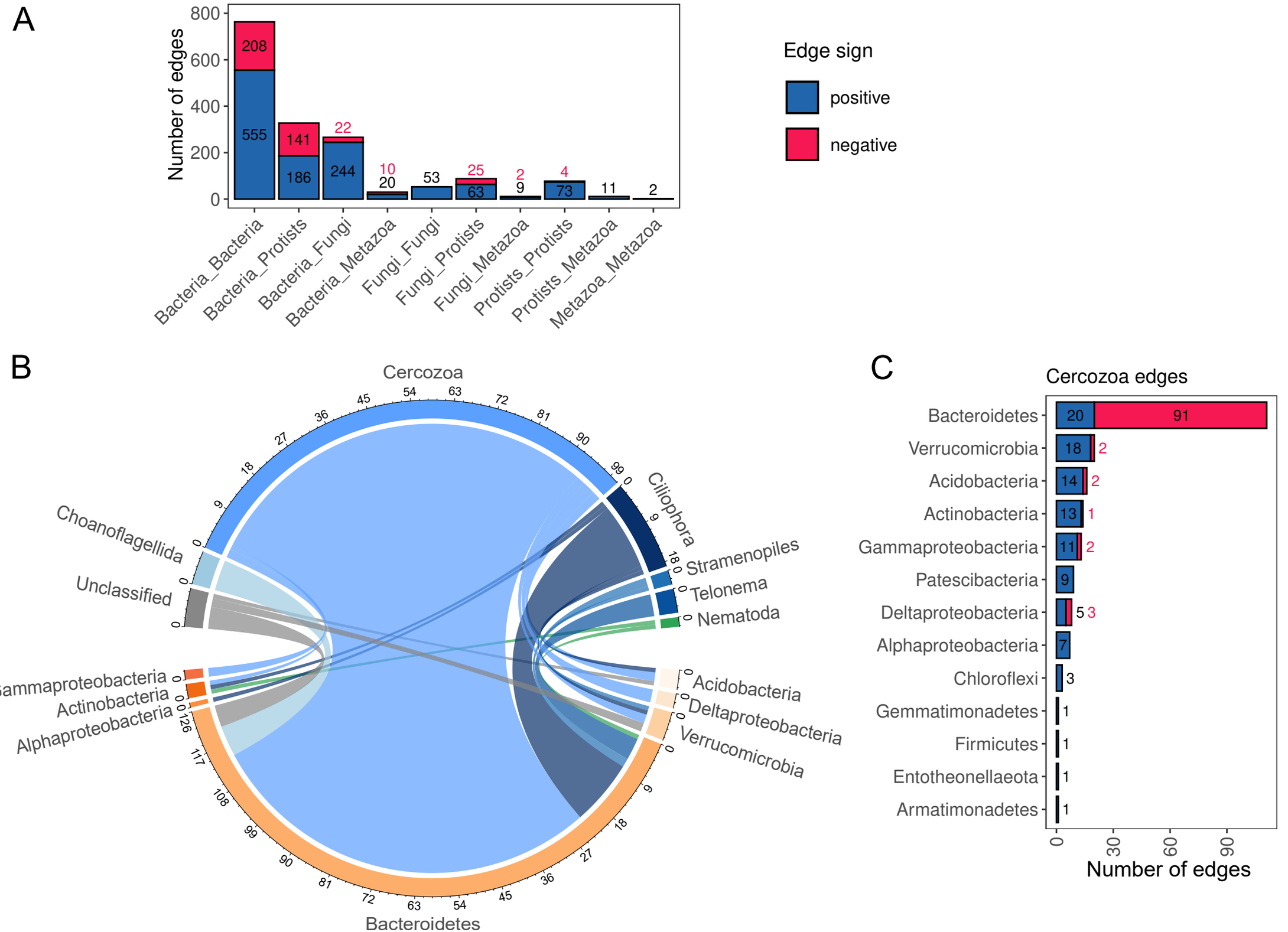
A
Number of edges
800
600
400
200
0
208
555
141
186
22
244
10
20
53
25
63
2
9
4
73
11
2
Bacteria_Bacteria
Bacteria_Protists
Bacteria_Fungi
Bacteria_Metazoa
Fungi_Fungi
Fungi_Protists
Fungi_Metazoa
Protists_Protists
Protists_Metazoa
Metazoa_Metazoa
Edge sign
positive
negative
B
Cercozoa
Ciliophora
Stramenopiles
Telonema
Nematoda
Choanoflagellida
Unclassified
Gammaproteobacteria
Actinobacteria
Alphaproteobacteria
Acidobacteria
Deltaproteobacteria
Verrucomicrobia
Bacteroidetes
C
Cercozoa edges
Bacteroidetes 20 91
Verrucomicrobia 18 2
Acidobacteria 14 2
Actinobacteria 13 1
Gammaproteobacteria 11 2
Patescibacteria 9
Deltaproteobacteria 5 3
Alphaproteobacteria 7
Chloroflexi 3
Gemmatimonadetes 1
Firmicutes 1
Entotheonellaeota 1
Armatimonadetes 1
0
30
60
90
Number of edges